

Transient Electro-Thermal Analysis of Dynamic Punch-Through in SiC Power Devices

W. Kaindl, M. Lades, G. Wachutka

*Institute for Physics of Electrotechnology, Munich University of Technology
Arcisstr. 21, 80290 Munich, Germany*

Abstract

Because of its rather large ionization energies compared to Si, dopants of SiC have larger ionization time constants. Therefore, dynamically enlarged space charge regions, eventually resulting in a punch-through (PT) situation in certain device structures, can easily occur. The detailed numerical analysis presented in this paper shows that the high currents caused by PT are able to destroy SiC power devices. As a consequence, the effect of dynamic PT has to be taken into account designing SiC devices.

1 Introduction

Due to its promising physical properties SiC has gained strong attention as alternative to Si for high power, high temperature, and high frequency applications [1]. Meanwhile, prototypes of all relevant devices are realized using SiC as basic material. However, due to the wide bandgap and the corresponding large ionization energies of the dopants, incomplete ionization sensitively affects the device operation and, therefore, has to be taken into account for an accurate device modeling [2]. Simulations based on measured ionization time constants of the most important dopants (N, Al, and B) for 4H- and 6H-SiC, respectively, reveal the effect of transient incomplete ionization on the switching behavior of power devices [3].

2 Modeling of the basic mechanism

The ionization time constants for electrons and holes, respectively,

$$\frac{1}{\tau_{n,p}} = \gamma_{n,p} \sigma_{n,p} T^2 \exp\left(-\frac{E_{D,A}}{kT}\right) \quad (1)$$

describe the emission of free carriers from donors and acceptors within a depletion region. $\gamma_{n,p}$ is a material parameter which is different for electrons and holes, respectively. The ionization time constants are mainly controlled by the energy level $E_{D,A}$ of the dopants and the capture cross section $\sigma_{n,p}$ for electrons and holes, respectively. These quantities were measured using DLTS and thermal admittance spectroscopy [4] (Fig. 1 right).

In order to demonstrate the relevance of dynamic incomplete ionization effects, respective rate equations have been incorporated in the multi-dimensional device simulator DESSIS-ISE [5] extending the electro-thermal drift-diffusion relations [6]. When a reverse bias pulse with a rise time smaller than the corresponding ionization time constant of

the dopants is applied to a pn-junction, the depletion region is dynamically enlarged (Fig.1 left) as first only that portion of dopants can contribute to the background charge which is ionized in thermal equilibrium. Within usual application temperatures, the rise times of bias pulses that can be achieved today are orders of magnitude larger than the ionization time constants for N and Al, respectively. In this case dynamic incomplete ionization effects are of second order. On the other hand, B dominated depletion regions can be drastically dynamically enlarged even at room temperature and above as B shows quite long ionization time constants compared to Al and N (Fig. 1 right).

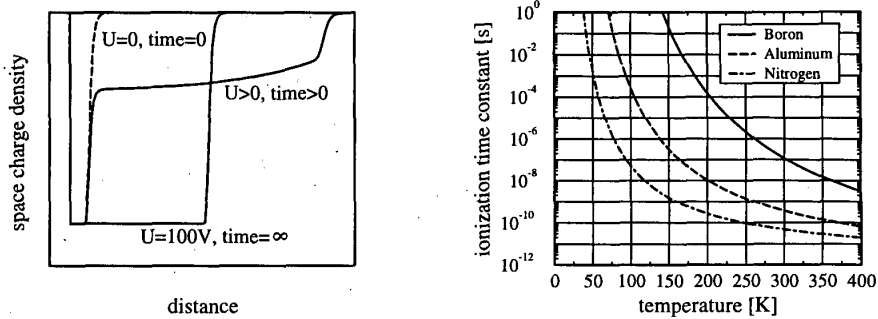


Figure 1: Simulation of dynamically enlarged depletion region (left) and measured temperature dependence of ionization time constants of 4H-SiC (right).

3 Simulation of dynamic punch-through

Considering active switching devices, the focus of interest today is on unipolar SiC power MOSFETs and JFETs. Because the critical field of SiC is nearly one order of magnitude higher compared to Si, the drift regions of SiC devices can be rather highly doped and shorter. Hence, the lower on-resistances lead to significant lower switching losses.

In back-to-back pn-junction configurations, the depletion region can touch the opposite n-layer leading to an abrupt rise of current (punch-through) [7]. An example for such a device containing a n^+pn^- -junction is the double implanted MOSFET (DIMOS) which has been reported in [8]. The principal structure is sketched on the left part of Fig. 2. In case of negligible ionization time constants, the voltage U_{PT_0} at which PT sets on is independent of temperature and pulse rise time. But if the ionization time constants are large, PT can occur at lower voltages than U_{PT_0} due to the dynamically enlarged depletion region.

The right part of Fig. 2 shows the simulated current transients obtained as response to a voltage ramp of -20V applied between source and drain at different temperatures. In order to demonstrate the current transients occurring during a dynamic PT, we simulated the built-in n^+pn^- -junction assuming the following test structure: a B base implantation with a $10^{16} \text{ cm}^{-3}/1.7 \mu\text{m}$ box profile and a N source implantation with a $10^{18} \text{ cm}^{-3}/0.5 \mu\text{m}$ box profile on a 10^{19} cm^{-3} N-doped layer. A negative bias pulse of -20V with a rise time of 10ns is applied to the source contact (see inset of right part of Fig. 2). Depending on the operating temperatures, we find a transient increase of the drain current setting on at voltages much smaller than U_{PT_0} because of the action of the dynamically ionized dopants. With decreasing temperatures the onset of PT is shifted towards lower voltages because of the larger ionization time constants and the resulting dynamical enlargement of the depletion region. The current transients after the end of the bias ramp are governed

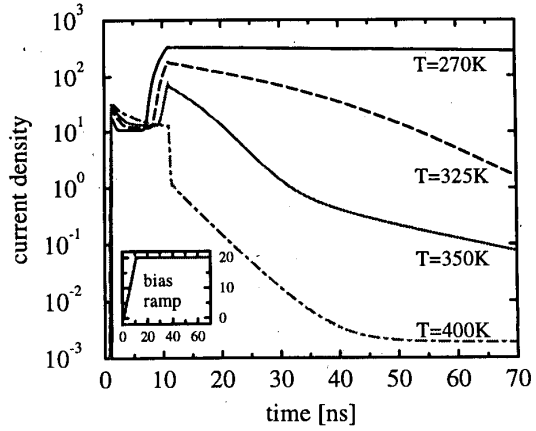
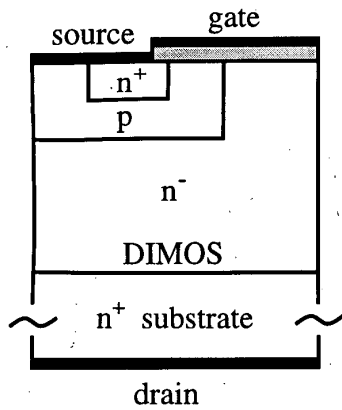


Figure 2: Structure of DIMOS cell (left) and simulated current transients (right).

by first by detaching the space charge region in the p-layer (e.g. $t=10-35\text{ns}$ for $T=350\text{K}$) and subsequently the ionization of the not yet ionized acceptors. This range ($t>35\text{ns}$, $T=350\text{K}$) is guided by the ionization time constant of B which could be extracted from the current transient. However, as the applied voltage and the resulting current response are relatively small, the total power loss density of 6 kW/cm^2 is not sufficient to damage the device within the applied time scale of several 10ns.

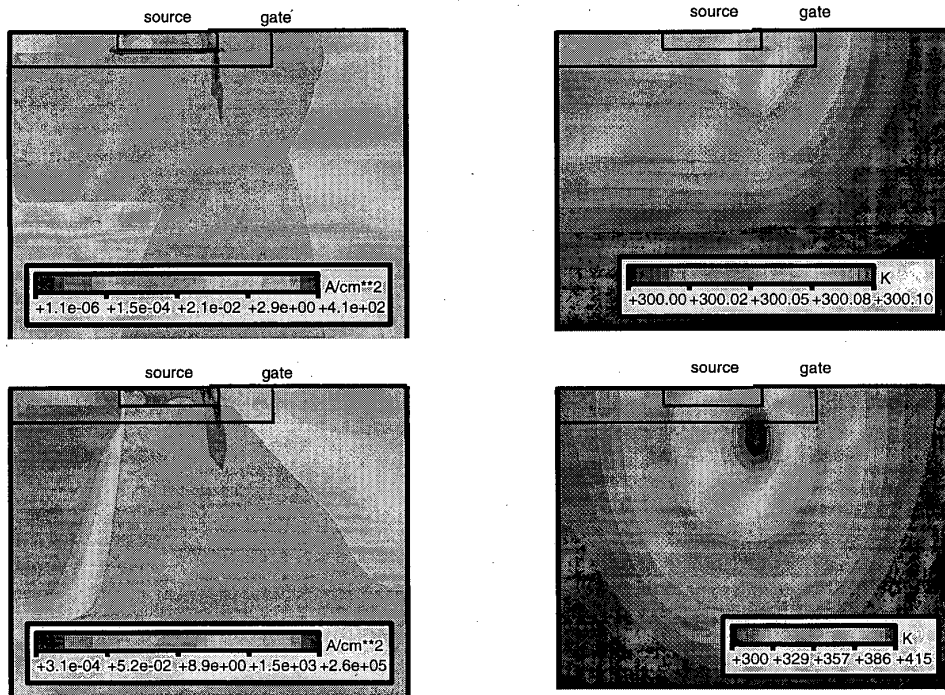


Figure 3: Distributions of current density (left) and temperature (right) during dynamic PT in a high power DIMOS. First row: onset of PT at -330V. Second row: formation of current filament at -500V.

A completely different situation occurs for the original DIMOS cell designed for high power operating conditions with, for instance, a B implantation doping profile of $N_A = 5 \cdot 10^{17} \text{ cm}^{-3}/1 \mu\text{m}$ and a N source implantation of $N_D = 10^{19} \text{ cm}^{-3}/0.5 \mu\text{m}$ in an epi-layer with a doping concentration of $N_D = 10^{16} \text{ cm}^{-3}$. Now the voltage at the source U_S is ramped up to -500V with a rise time of 100ns. Dynamic PT sets on at a voltage of about -330V at 300K.

In order to give insight into this situation, internal data of the device is analyzed. A snapshot of distributions of current density and temperature at the onset of PT is shown in the upper parts of Fig. 3. A current filament starts to form in the vicinity of the n^+p -junction. There is also a slight increase of temperature at this location, but the overall temperature rise is still insignificant. As the voltage is further increasing beyond $U_S = -330\text{V}$ the filament is rapidly growing and generates a hot spot near the junction (second row of Fig. 3). While the voltage is kept constant after reaching the final value of -500V, the temperature of the hot spot climbs up to 1000K. The current transients show qualitatively the same evolution as in the "low-power" example (Fig. 2 right) up to the instant when temperature starts rising. Of course, under such extreme operating conditions a qualitative analysis becomes problematic, since the validity of the underlying physical models is doubtful in the high temperature range. But despite of potential inaccuracies, the qualitative behavior of the failure process is nevertheless correctly described: With an estimated power loss density of about $1.5 \text{ GW}/\text{cm}^2$, we can conclude that this is sufficient to cause localized melting within the hot spot. Hence, dynamic PT will lead to the destruction of the device.

4 Conclusion

Based on the extended drift-diffusion model we investigated the effect of dynamically enlarged depletion regions leading to PT in back-to-back structures. We identified dynamic PT as a possible destruction mechanism in SiC power devices. The high currents and the resulting high temperatures are able to cause localized melting of the device. As a consequence, the effect of dynamic PT has to be taken into account designing new SiC devices.

The authors are grateful to N. Kaminski for providing helpful advice and the ISE for providing software facilities.

References

- [1] J.B. Casady, and R.W. Johnson, *Solid-State Electron.*, vol. 39, pp. 1409-1422, 1996.
- [2] G. Wachutka, *Microelectronics Journal*, vol. 26, pp. 307-315, 1995.
- [3] M. Lades, W. Kaendl, N. Kaminski, E. Niemann, G. Wachutka, *IEEE Trans. on Elec. Dev.*, special issue on SiC, vol. 46(3), pp. 598-604, 1999.
- [4] W. Kaendl, M. Lades, N. Kaminski, E. Niemann, G. Wachutka, *Jour. Elec. Mat.*, special issue on SiC, vol. 28(3), pp. 154-160, 1999.
- [5] ISE Integrated Systems Engineering AG, 1996.
- [6] M. Lades, G. Wachutka, *Proc. of SISPAD'98*, Springer Verlag, pp. 251-254, 1998.
- [7] S.M. Sze, "Physics of Semiconductor Devices", John Wiley, 1981.
- [8] J.N. Shenoy, J.A. Cooper, M.R. Melloch, *IEEE Elec. Dev. Let.*, vol. 18, pp. 93-95, 1997.